A pattern-based technique for ground-roll and multiple attenuation

Antoine Guitton, Morgan Brown, James Rickett, and Robert Clapp[1]

ABSTRACT

We present a pattern-based method that separates coherent noise from signal. This method finds its mathematical foundation in the work conducted by Nemeth (1996) on coherent noise attenuation by least-squares migration. We show that a similar inverse problem can be formulated to attenuate coherent noise in seismic data. In this paper, we use deconvolution with prediction error filters to model the signal and noise vectors in a least-squares sense. This new formulation of the noise separation problem has been tested on 2-D real data for ground-roll and multiple attenuations. So far, it achieves similar results to the approach used by Brown and Clapp (2000) and Clapp and Brown (2000). However, we show that the main strength of this new method is its ability to incorporate regularization in the inverse problem in order to decrease the correlation effects between noise and signal.

INTRODUCTION

This paper introduces a noise attenuation method based on the recognition of coherent events. Because this method exploits the spatial predictability of the noise and signal with prediction error filters (PEF), it belongs to the family of pattern-based techniques (Spitz, 2000; Brown and Clapp, 2000). Pattern-based noise attenuation techniques are known for their ability to remove coherent noise in the most complex geology (Guitton, 1999). They also assume advance knowledge of a noise model, which might be rather difficult to derive in many situations. However, in some circumstances, a noise model can be calculated. For example, we can derive a multiple model using the "Delft approach" (Verschuur et al., 1992) in which the multiple model is calculated via autoconvolution of the recorded wavefield. For ground-roll attenuation, Brown et al. (1999) demonstrate that a satisfactory model can be obtained by low-passing the data.

The recent pattern-based techniques in the literature are approximately equivalent to Wiener optimal estimation (Castleman, 1996) since they utilize the PEF to approximate the signal and noise power spectra. For instance, Spitz (2000) uses $f-x$ domain PEF while Brown and Clapp (2000) and Clapp and Brown (2000) use $t-x$ domain PEF.

[1]**email:** antoine@sep.stanford.edu, morgan@sep.stanford.edu, james@sep.stanford.edu, bob@sep.stanford.edu

In this report, Guitton (2001) presents a method that is not based on the Wiener reconstruction of the signal but that still uses $t-x$ domain PEF. Following Guitton's idea, we use the PEFs as prediction operators as opposed to filtering operators in the Wiener approach. Nonetheless, this method belongs to the pattern-based type since PEFs are still estimated for the noise separation. Our goal is to show that this new methodology leads to a proper attenuation of ground-roll and multiples, and has the potential to rival the classical Wiener formulation.

In the first part of this paper, we briefly review the theoretical developments of both the Wiener-like scheme and the new proposed technique, discussing their differences and similarities. Then, we compare the two strategies applied to a 3-D shot gather infested with ground-roll, and multiple-infested CMP gathers in a region of complex geology.

THEORY REVIEW

We present the theoretical basis for both the Wiener method and the new proposed scheme. We show that our new method offers the opportunity to better separate noise from signal using inverse theory.

Wiener-like method

A constrained least-squares problem using PEFs gives a similar expression for the noise estimation to the Wiener method. To see this, consider the recorded data to be the simple superposition of signal and noise, that is $\mathbf{d}=\mathbf{s}+\mathbf{n}$. For the special case of uncorrelated signal and noise, the so-called *Wiener estimator*, is a filter which when applied to the data, yields an optimal (in a least-squares sense) estimate of the embedded signal (Castleman, 1996). The frequency response of this filter is

$$\mathbf{H}=\frac{\mathbf{P_s}}{\mathbf{P_n}+\mathbf{P_s}}, \tag{1}$$

where $\mathbf{P_s}$ and $\mathbf{P_n}$ are the signal and noise power spectra, respectively.

Similarly, Abma (1995) solved a constrained least squares problem to separate signal from spatially uncorrelated noise:

$$\begin{aligned} \mathbf{Nn} &\approx 0 \\ \epsilon\mathbf{Ss} &\approx 0 \\ \text{subject to} &\leftrightarrow \mathbf{d}=\mathbf{s}+\mathbf{n} \end{aligned} \tag{2}$$

where the operators $\mathbf{N}$ and $\mathbf{S}$ represent $t-x$ domain convolution with nonstationary PEF which whiten the unknown noise $\mathbf{n}$ and signal $\mathbf{s}$, respectively, and ϵ is a Lagrange multiplier. Minimizing the quadratic objective function suggested by equation (2) with respect to $\mathbf{s}$ leads to the following expression for the estimated signal:

$$\hat{\mathbf{s}}=\left(\mathbf{N^T N}+\epsilon^2\mathbf{S^T S}\right)^{-1}\mathbf{N^T N}\,\mathbf{d} \tag{3}$$

By construction, the frequency response of a PEF approximates the inverse power spectrum of the data from which it was estimated. Thus we see that the approach of equation (2) is similar to the Wiener reconstruction process. We refer to this approach as a "Wiener-like" method. It has been successfully used by Brown and Clapp (2000) for ground-roll attenuation and by Clapp and Brown (2000) for multiple separation.

Subtraction method

In contrast to the Wiener-like method which filters the noise, the following method aims to model the noise and then subtract it from the input data. In this section, we show that the formalism used by Nemeth (1996) can help to better separate correlated noise and signal. But first, we detail the similarities and differences between the Wiener-like and the subtraction method.

In equation (2), the noise and signal PEFs filter the data components. Alternatively, building on Nemeth (1996), the noise and signal nonstationary PEF can predict the data components via a deconvolution as follows:

$$\mathbf{d} = \mathbf{N^{-1}m_n} + \mathbf{S^{-1}m_s}. \tag{4}$$

We call $\mathbf{m_s}$ the signal model component and $\mathbf{m_n}$ the noise model component (not to be confused with the noise model that we use to compute the noise PEF). Clearly, $\mathbf{N^{-1}m_n}$ models the noise vector $\mathbf{n}$ and $\mathbf{S^{-1}m_s}$ the signal vector $\mathbf{s}$. Because we use PEFs in equation (4), this approach is pattern-based in essence. With $\mathbf{L_n} = \mathbf{N^{-1}}$ and $\mathbf{L_s} = \mathbf{S^{-1}}$, using linear algebra, we can prove that the least-squares solution of $\mathbf{m_s}$ and $\mathbf{m_n}$ is

$$\begin{pmatrix} \hat{\mathbf{m}}_\mathbf{n} \\ \hat{\mathbf{m}}_\mathbf{s} \end{pmatrix} = \begin{pmatrix} (\mathbf{L_n'}\overline{\mathbf{R_s}}\mathbf{L_n})^{-1}\mathbf{L_n'}\overline{\mathbf{R_s}} \\ (\mathbf{L_s'}\overline{\mathbf{R_n}}\mathbf{L_s})^{-1}\mathbf{L_s'}\overline{\mathbf{R_n}} \end{pmatrix} \mathbf{d}, \tag{5}$$

with

$$\begin{aligned} \overline{\mathbf{R_s}} &= \mathbf{I} - \mathbf{L_s}(\mathbf{L_s'L_s})^{-1}\mathbf{L_s'}, \\ \overline{\mathbf{R_n}} &= \mathbf{I} - \mathbf{L_n}(\mathbf{L_n'L_n})^{-1}\mathbf{L_n'}. \end{aligned} \tag{6}$$

The operators $\overline{\mathbf{R_s}}$ and $\overline{\mathbf{R_n}}$ can be seen as signal and noise filters respectively since $\mathbf{L_s}(\mathbf{L_s'L_s})^{-1}\mathbf{L_s'}$ and $\mathbf{L_n}(\mathbf{L_n'L_n})^{-1}\mathbf{L_n'}$ are the data resolution operators for the signal and the noise, respectively. In the appendix B, we give a geometrical interpretation for both $\overline{\mathbf{R_s}}$ and $\overline{\mathbf{R_n}}$.

The degree of orthogonality between the noise operator $\mathbf{L_n}$ and the signal operator $\mathbf{L_s}$ restricts the existence of $\hat{\mathbf{m}}_\mathbf{n}$ and $\hat{\mathbf{m}}_\mathbf{s}$ in equation (5). If the two operators overlap completely, the Hessians $\mathbf{L_n'}\overline{\mathbf{R_s}}\mathbf{L_n}$ and $\mathbf{L_s'}\overline{\mathbf{R_n}}\mathbf{L_s}$ are not invertible. If the two operators overlap only partially, Nemeth (1996) proves that the separability of the signal and noise can be improved if we introduce a regularization term. If we use a model space regularization (Fomel, 1997), we have

$$\begin{pmatrix} \hat{\mathbf{m}}_\mathbf{n} \\ \hat{\mathbf{m}}_\mathbf{s} \end{pmatrix} = \begin{pmatrix} (\mathbf{L_n'}\overline{\mathbf{R_s}}\mathbf{L_n} + \epsilon^2\mathbf{C_n'C_n})^{-1}\mathbf{L_n'}\overline{\mathbf{R_s}} \\ (\mathbf{L_s'}\overline{\mathbf{R_n}}\mathbf{L_s} + \epsilon^2\mathbf{C_s'C_s})^{-1}\mathbf{L_s'}\overline{\mathbf{R_n}} \end{pmatrix} \mathbf{d}, \tag{7}$$

with $\mathbf{C_n}$ and $\mathbf{C_s}$ the regularization operators for the noise model $\mathbf{m_n}$ and the signal model $\mathbf{m_s}$. A data space regularization can also improve the separation but will not be considered here.

In equation (4), the outcome of the inversion is $\mathbf{m_n}$ and $\mathbf{m_s}$. The estimated signal $\tilde{\mathbf{s}}$ is then easily derived as follows:

$$\tilde{\mathbf{s}} = \mathbf{d} - \mathbf{N}^{-1}\mathbf{m_n}. \tag{8}$$

We call this new method the subtraction method. In the next two sections, we compare the Wiener-like approach and the subtraction method for ground-roll and multiple attenuation.

Approximating the signal PEF

In this section, we describe a method that computes the signal PEF needed in equations (2) and (4). Spitz (1999) showed that for uncorrelated signal and noise, the signal PEF can be expressed in terms of 2 PEF's: a PEF **D**, estimated from the data **d**, and a PEF **N**, estimated from the noise model such that

$$\mathbf{S} = \mathbf{D}\mathbf{N}^{-1}. \tag{9}$$

Equation (9) states that the signal PEF equals the data PEF deconvolved by the noise PEF. Spitz formulated the problem in the $f-x$ domain, but the helix transform (Claerbout, 1998) permits stable inverse filtering with multidimensional $t-x$ domain filters.

COHERENT NOISE ATTENUATION RESULTS

We present coherent noise attenuation results when ground-roll and multiples are present in the data. These results prove that at this stage, the subtraction technique compares favorably to the Wiener-like method. So far, we did not incorporate a regularization term as suggested above.

Attenuation of ground-roll

The first test aims to attenuate severely aliased hyperbolic ground-roll. The shot gather in Figure 1a comes from a 3-D land acquisition survey in Saudi Arabia. This shot gather has been previously used by Brown et al. (1999) and Fomel (2000). With this field example, because the noise and the signal span distinct frequency bandwiths, the ground-roll may be attenuated by applying a high-pass filter. However, Fomel (2000) shows that the separation in that case is far from optimal. Nonetheless, a low-pass filtering of the data gives an excellent ground-roll model that can be later used for the coherent noise attenuation. Figure 1b shows the noise model obtained with a bandpass filter. We added random noise to the noise model in order to stabilize the PEF inversion. We then estimated the noise PEFs **N** from this model.

After building the noise model, we performed the coherent noise attenuation using the two preceding schemes (equations (2) and (4)). The PEF and patch sizes are different in the two

cases. With this dataset, we noticed that a larger PEF was needed in the subtraction scheme. The number of iterations needed in the PEF estimation and in the final inversion is the same for both methods. The parameters used in the Wiener-like technique are directly taken from Brown et al. (1999) and correspond to the best possible combination of parameters for an optimal separation of the noise from the signal.

Figure 2 shows the result of the noise attenuation for both methods. The two panels look similar and both show that the ground-roll has been correctly separated from the signal. Figure 3 shows the estimated noise computed by subtracting the signal in Figure 2 from the input data in Figure 1a. We see that the subtraction did a better job at preserving the signal because few coherent events remain outside the ground-roll cone in the estimated noise panel in Figure 3a.

Attenuation of multiples

We use the very popular Gulf of Mexico line provided by WesternGeco. In the middle of the seismic section shown in Figure 4, the data contain a shallow salt body which generates strong reverberations and diffractions. This dataset is frequently utilized to benchmark multiple attenuation techniques.

The multiple model was calculated in the shot domain using a non-recursive version of the SRME technique developed by Delft (Verschuur et al., 1992). We describe how we created the multiple model in the appendix A [equation (16)]. In few words, the goal of our modeling algorithm is to generate a kinematically correct multiple field. Therefore, there is no attempt to compensate for source signature effects. Indeed, our hope is that the attenuation scheme is robust enough to cope with significant amplitude errors in the multiple model. Figure 5 shows a comparison between one recorded shot gather on the right, and the multiple model for the same shot location on the left. This shot is taken at the vertical of the salt body. The kinematics of the input data, displayed in the right-hand panel of Figure 5, are accurately reproduced in the multiple model (left-hand panel of Figure 5). The missing energy at near offset in the multiple model results from the lack of short offset traces. Out-of-plane effects might affect the accuracy of the model considerably. In addition, the limited aperture of the recording geometry may cause modeling problems when dipping beds are present in the subsurface (Guitton, 1999).

The multiple prediction is done in the shot domain, but our multiple attenuation scheme was tested in the CMP domain. The next two sections present multiple attenuation results for one CMP gather outside the salt boundaries and one over the salt body.

Figure 6a shows a CMP gather extracted from the Gulf of Mexico dataset, outside the salt boundaries, and infested with multiples. Figure 6b shows the multiple model at the same location. The main patterns are accurately modeled but the relative amplitudes of high-order multiples are not preserved. The multiple attenuation starts by estimating the PEF for the data and the noise model. The PEF coefficients are then smoothed along radial directions to stabilize their inversion (Clapp et al., 1999). Then, the noise attenuation begins with either equation (2), for the Wiener-like method, or equation (4), for the subtraction scheme. Figure

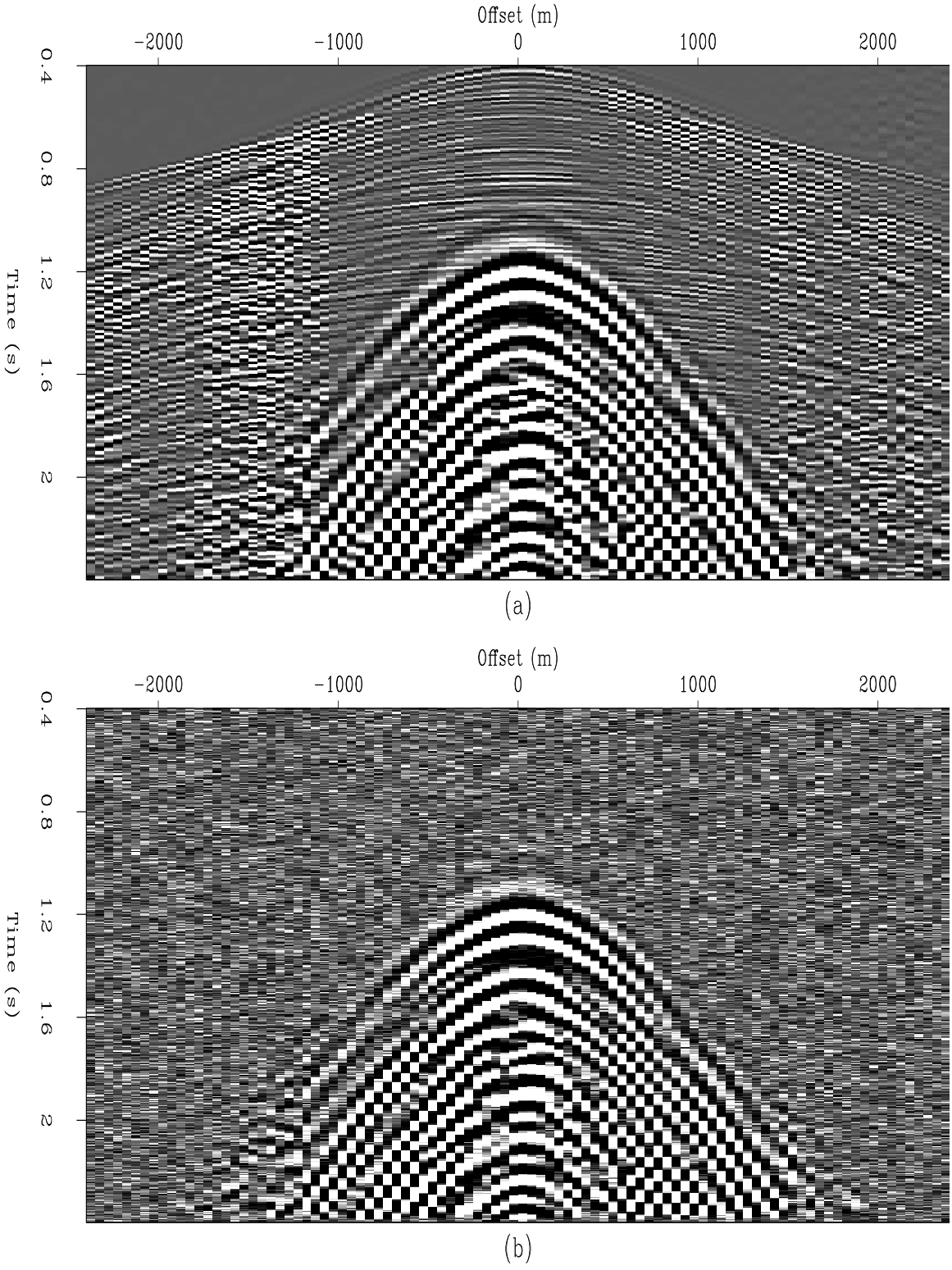

Figure 1: (a) Ground-roll contaminated shot gather. (b) The ground-roll model used to compute the noise PEF **N** (low pass filter of a, plus random noise). antoine2-dune [ER]

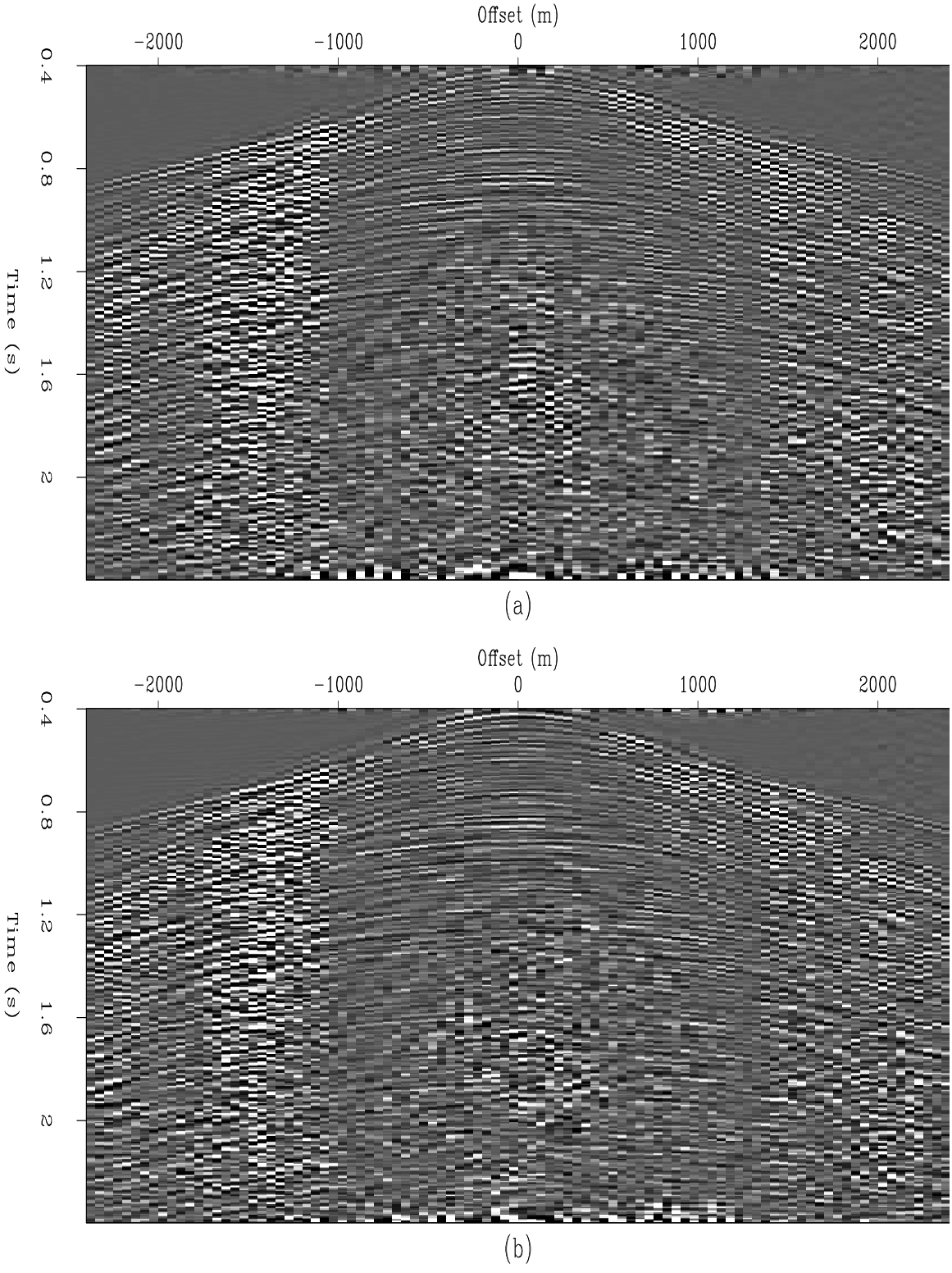

Figure 2: (a) The estimated signal using the subtraction scheme. (b) The estimated signal using the Wiener-like method. Both results are very similar. antoine2-dune-signal [ER]

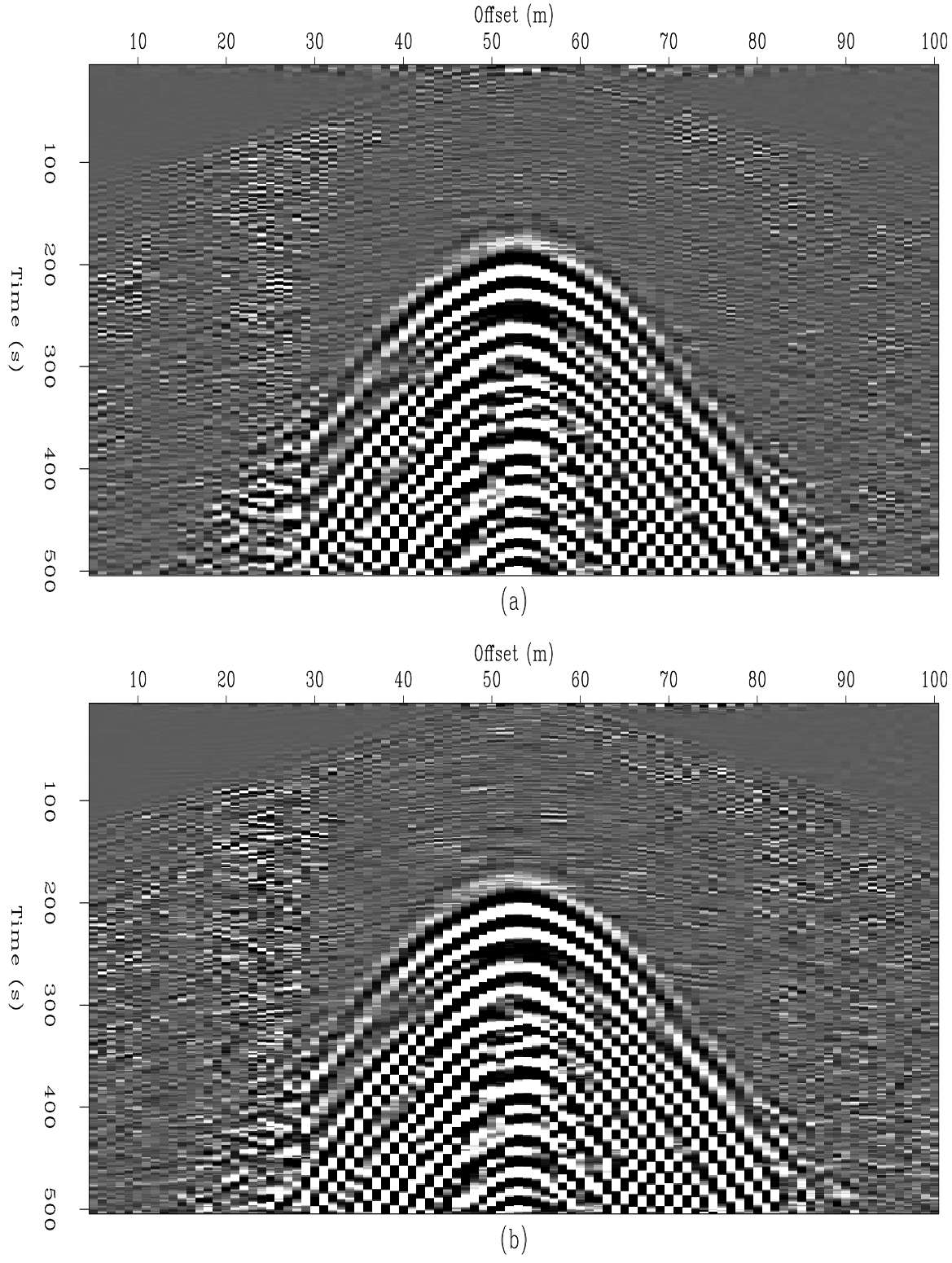

Figure 3: (a) The estimated noise using the subtraction scheme. (b) The estimated signal using the Wiener-like method. Less coherent noise is left outside the ground-roll cone for the subtraction method. antoine2-dune-noise [ER]

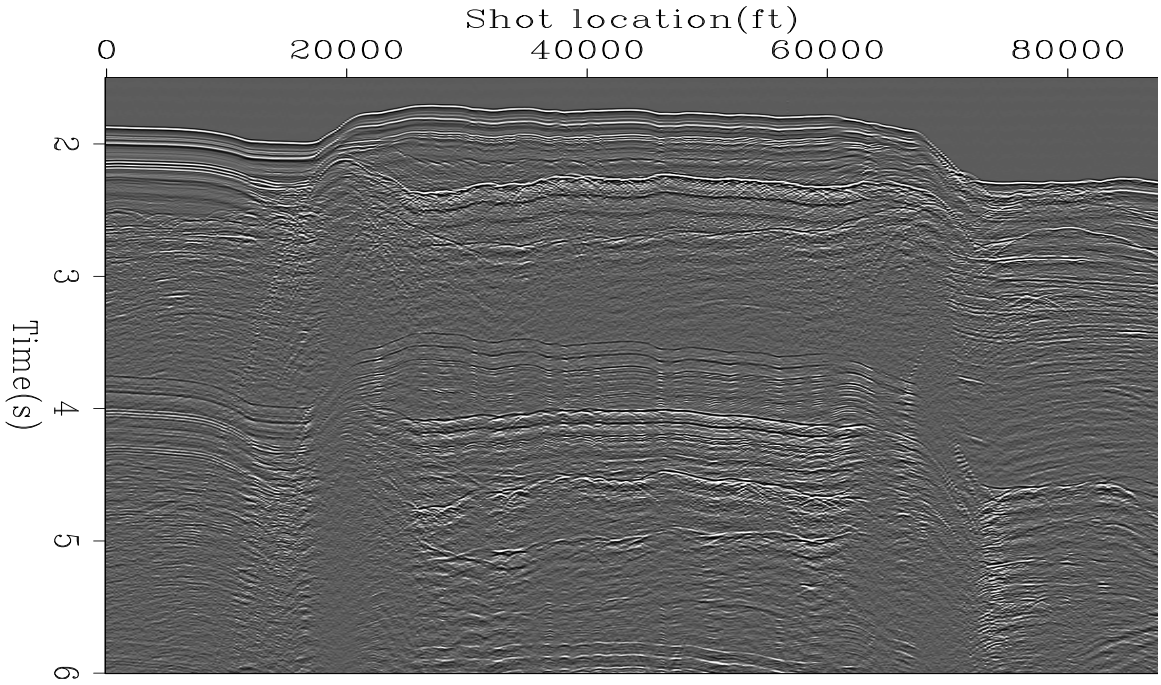

Figure 4: Zero-offset section of the Gulf of Mexico data showing strong water-column multiples below 3.5 seconds. antoine2-zero-offset [ER]

7 displays the result of the multiple attenuation using both methods. The multiples have been correctly attenuated in the two cases. Figure 8 shows the difference between the input data and the multiple-free gather using both methods. The two noise attenuation schemes lead to very similar results.

For the last multiple attenuation result of this paper, we extracted a CMP gather over the salt body. Multiple attenuation becomes more challenging because the salt body generates strong internal multiples, diffractions and shadow zones that are difficult to incorporate in the noise model. Figure 9 shows the selected CMP gather inside the salt boundaries with the corresponding multiple model. Despite the inherent difficulty of modeling subsalt multiples, the kinematics of the multiples in Figure 9a look similar to those in Figure 9b. Figure 10 shows the estimated signal. As expected, the remaining signal is less coherent inside the salt boundaries than outside. Nonetheless, the two schemes reveal hidden information in a similar way. Figure 11 proves that once again, the coherent noise attenuation is comparable for both methods.

CONCLUSION

We applied a new $t-x$ domain, pattern-based signal/noise separation technique to a 2-D line contaminated with multiples. This technique differs from the Wiener-like method because the data components are not filtered but rather predicted. The goal of this work was to show (1) that the noise attenuation can be formulated in a totally different way using a new fitting goal,

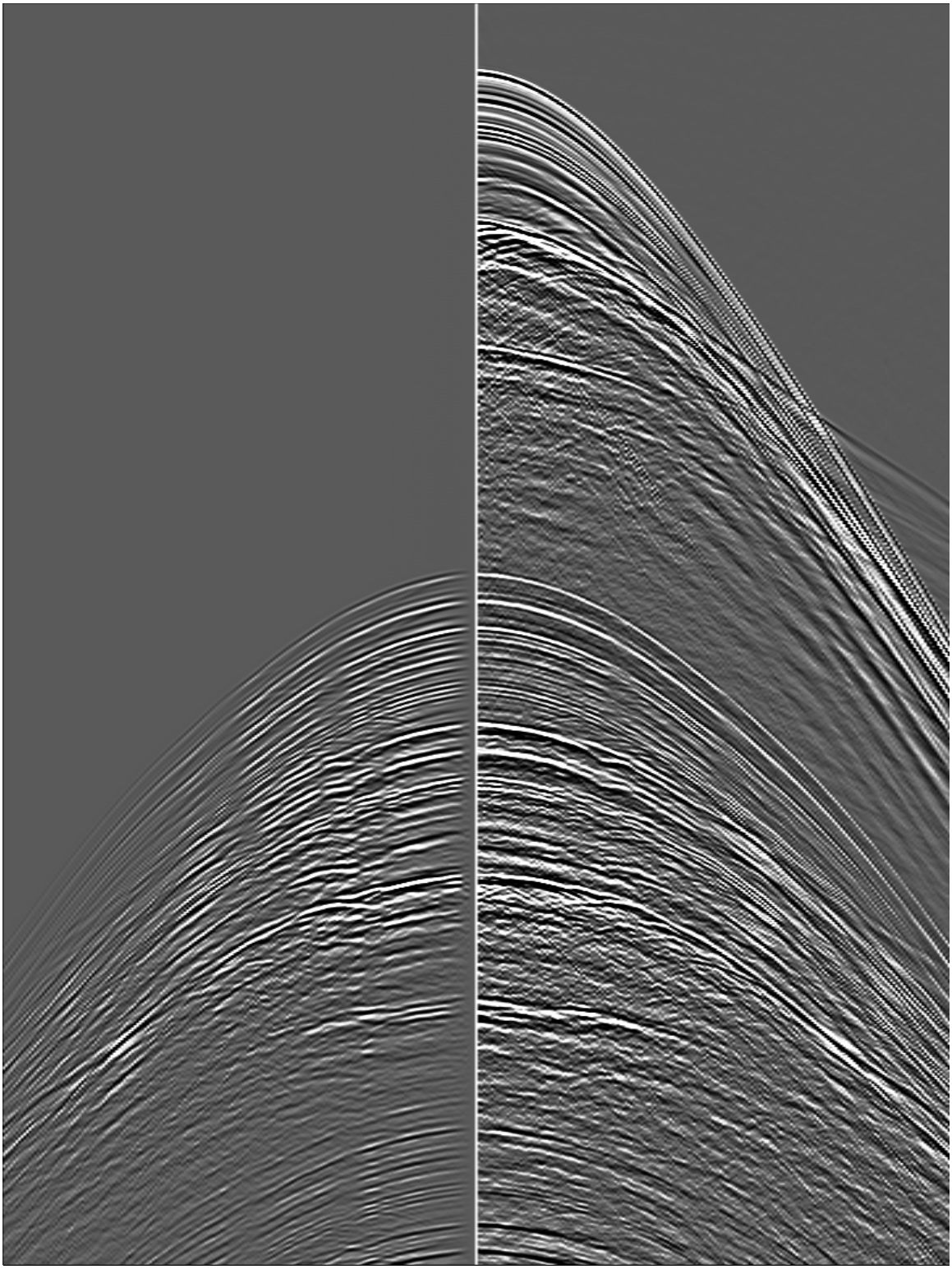

Figure 5: Left: A multiple model at one shot location. Right: The shot record at the same location. The multiple model matches the recorded multiples accurately. antoine2-comp [CR]

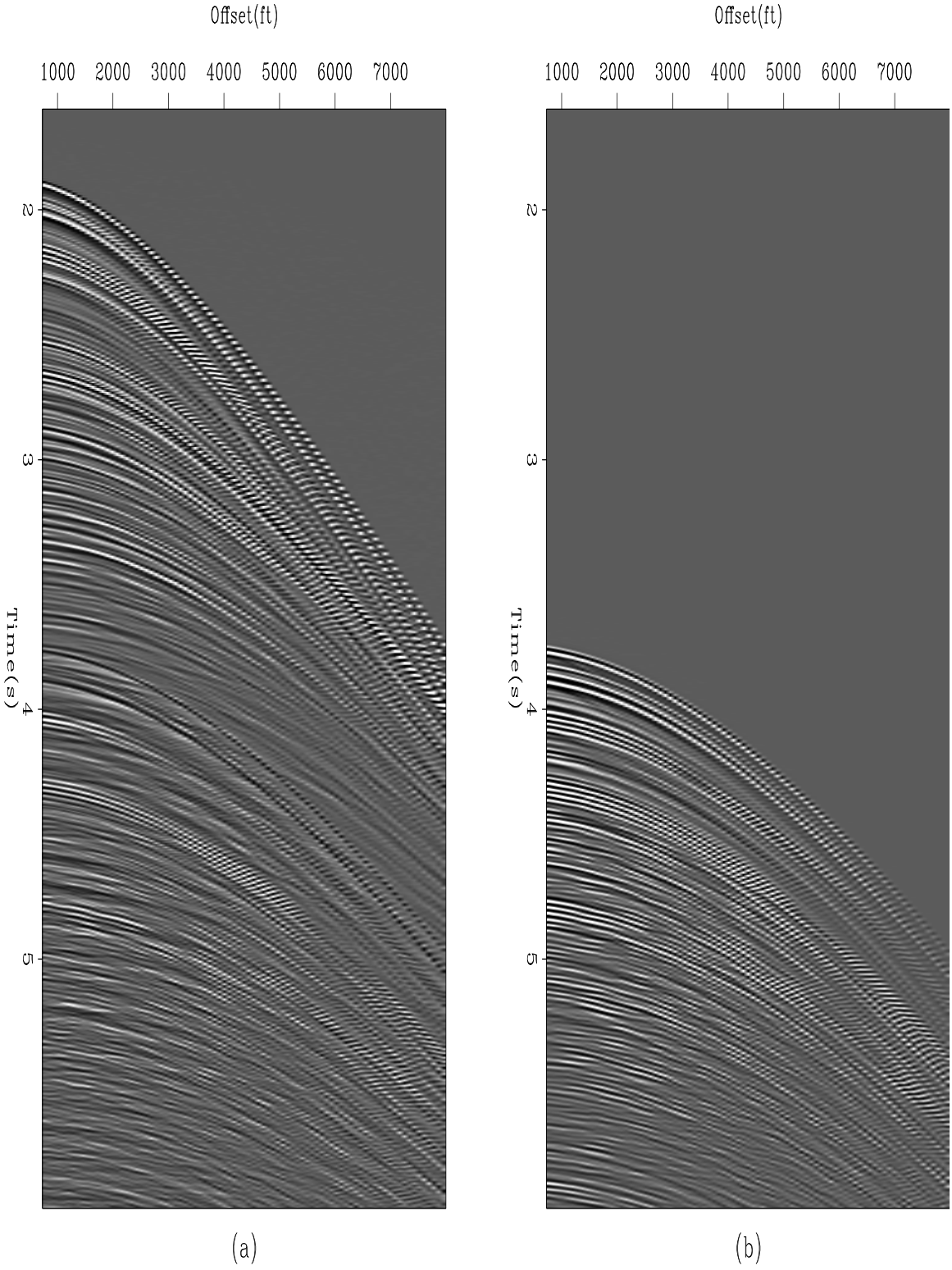

Figure 6: (a) A CMP gather infested with multiples, outside the salt boundaries. (b) The multiple model at the same location. antoine2-inp-1 [CR]

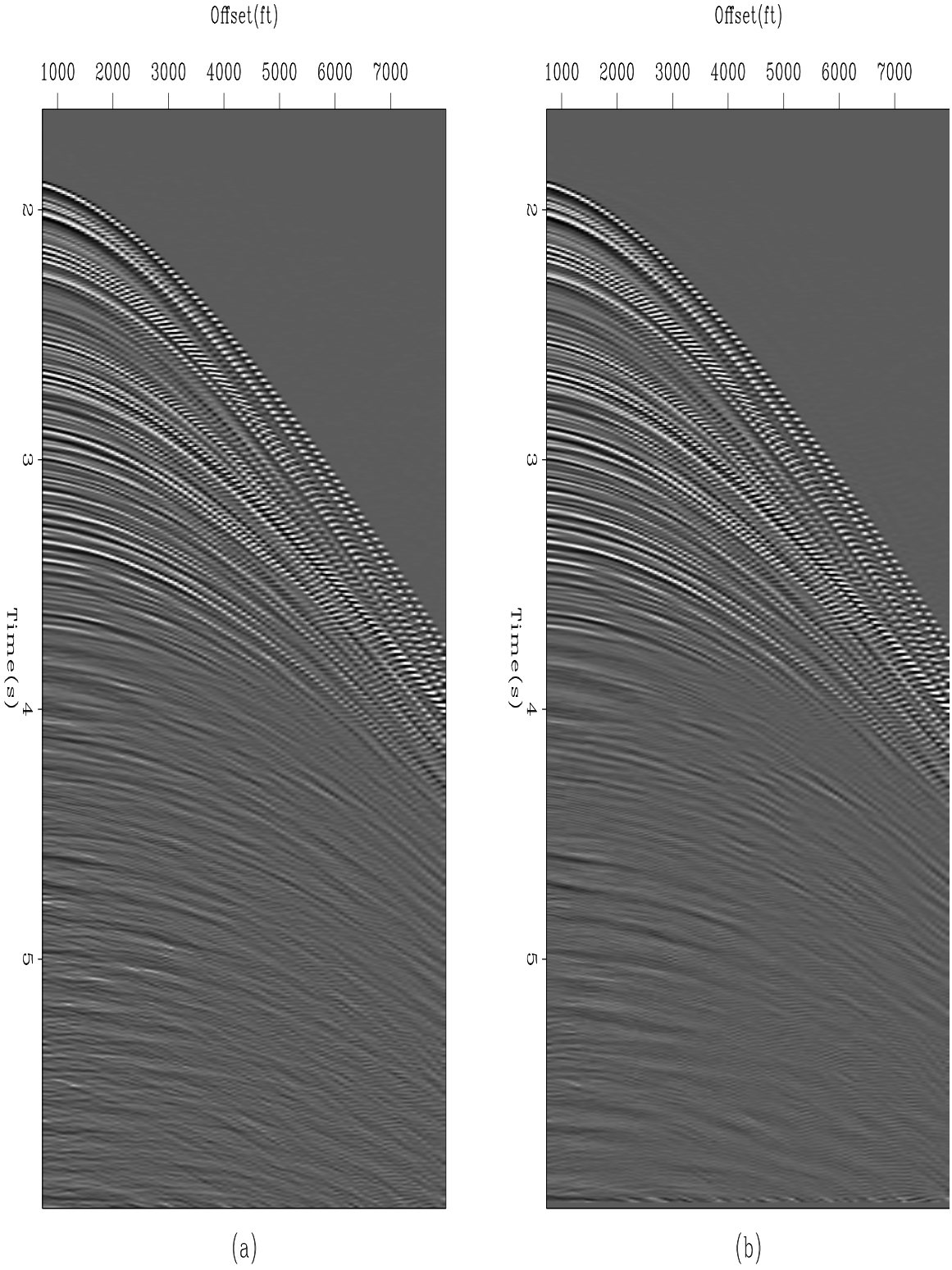

Figure 7: (a) The estimated signal using the subtraction method. (b) The estimated signal using the Wiener-like method. Both results are comparable. antoine2-sig-1 [CR]

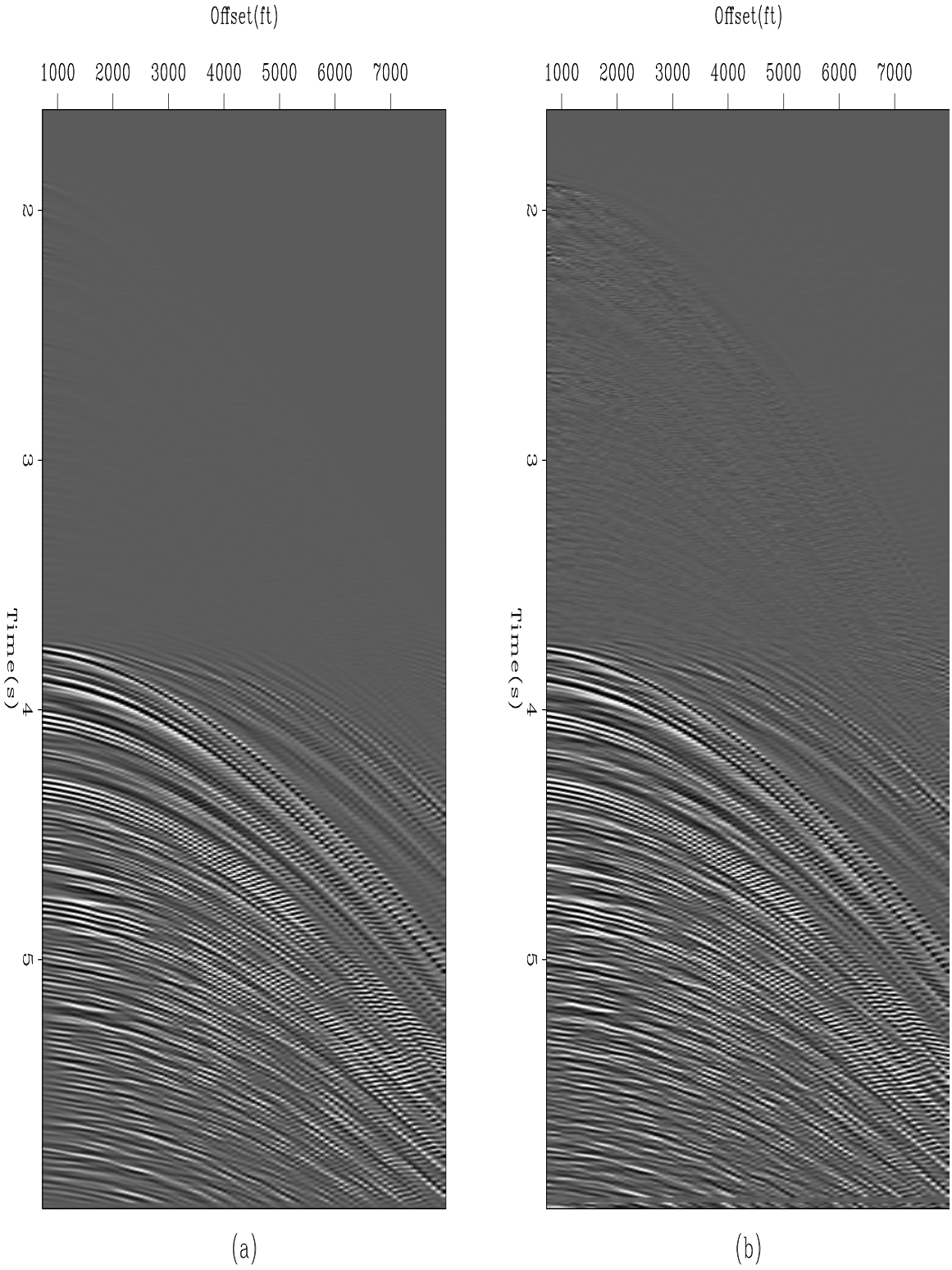

Figure 8: (a) The extracted multiples using the subtraction method. (b) The extracted multiples using the Wiener-like method. The noise attenuation is similar in both cases. antoine2-noiz-1 [CR]

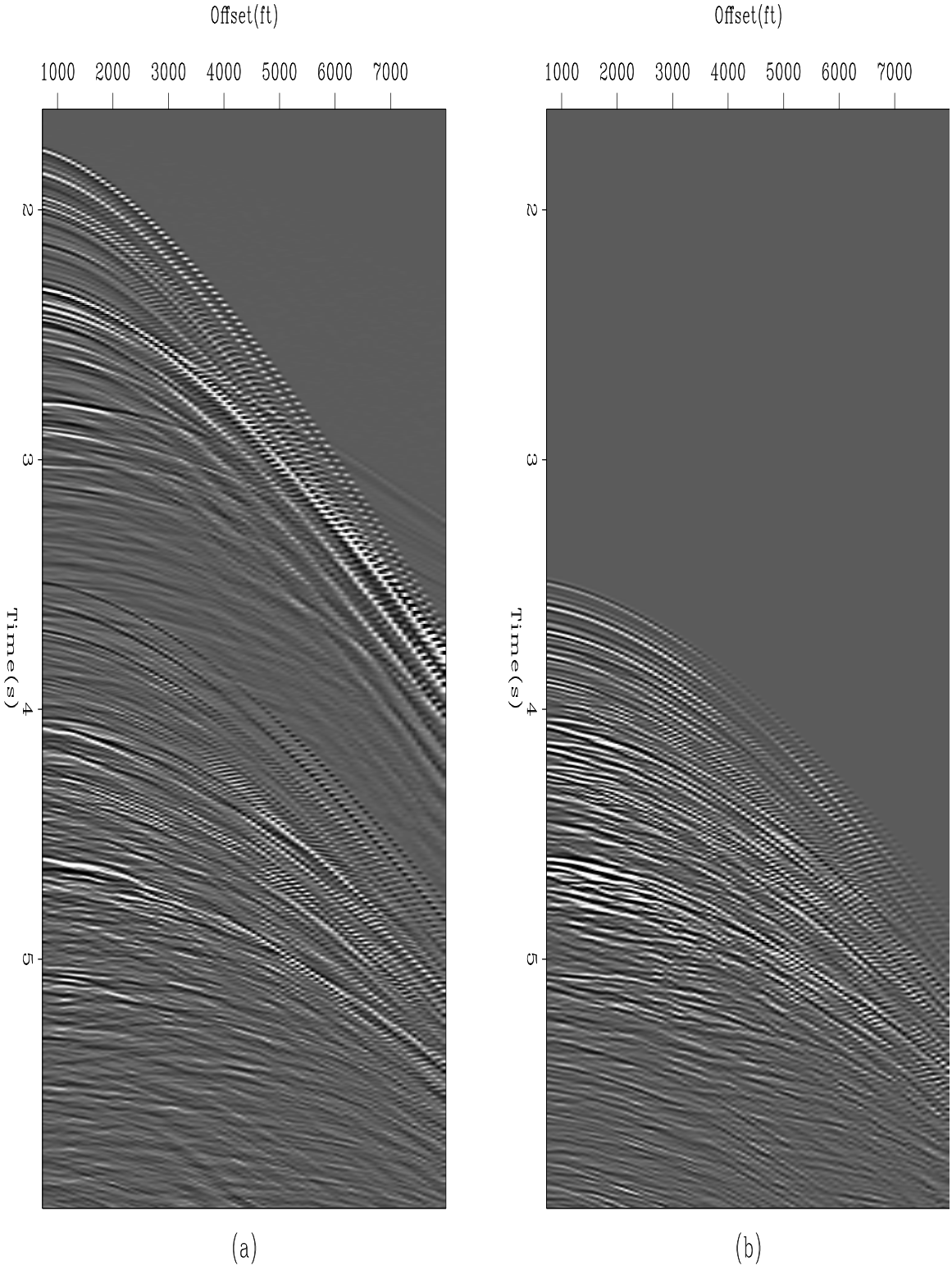

Figure 9: (a) A CMP gather infested with multiples, inside the salt boundaries. (b) The multiple model at the same location. antoine2-inp-400 [CR]

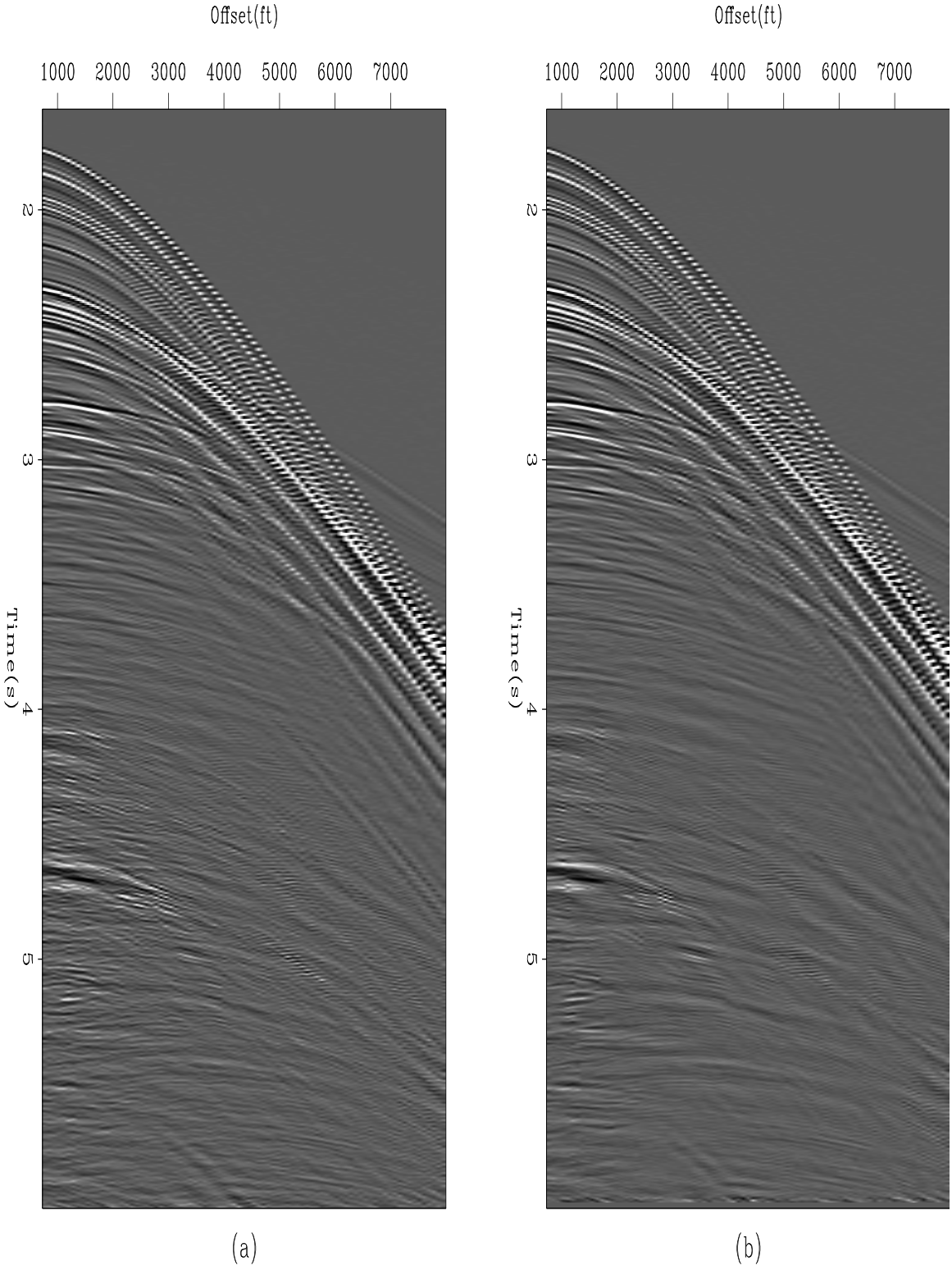

Figure 10: (a) The estimated signal using the subtraction method. (b) The estimated signal using the Wiener-like method. antoine2-sig-400 [CR]

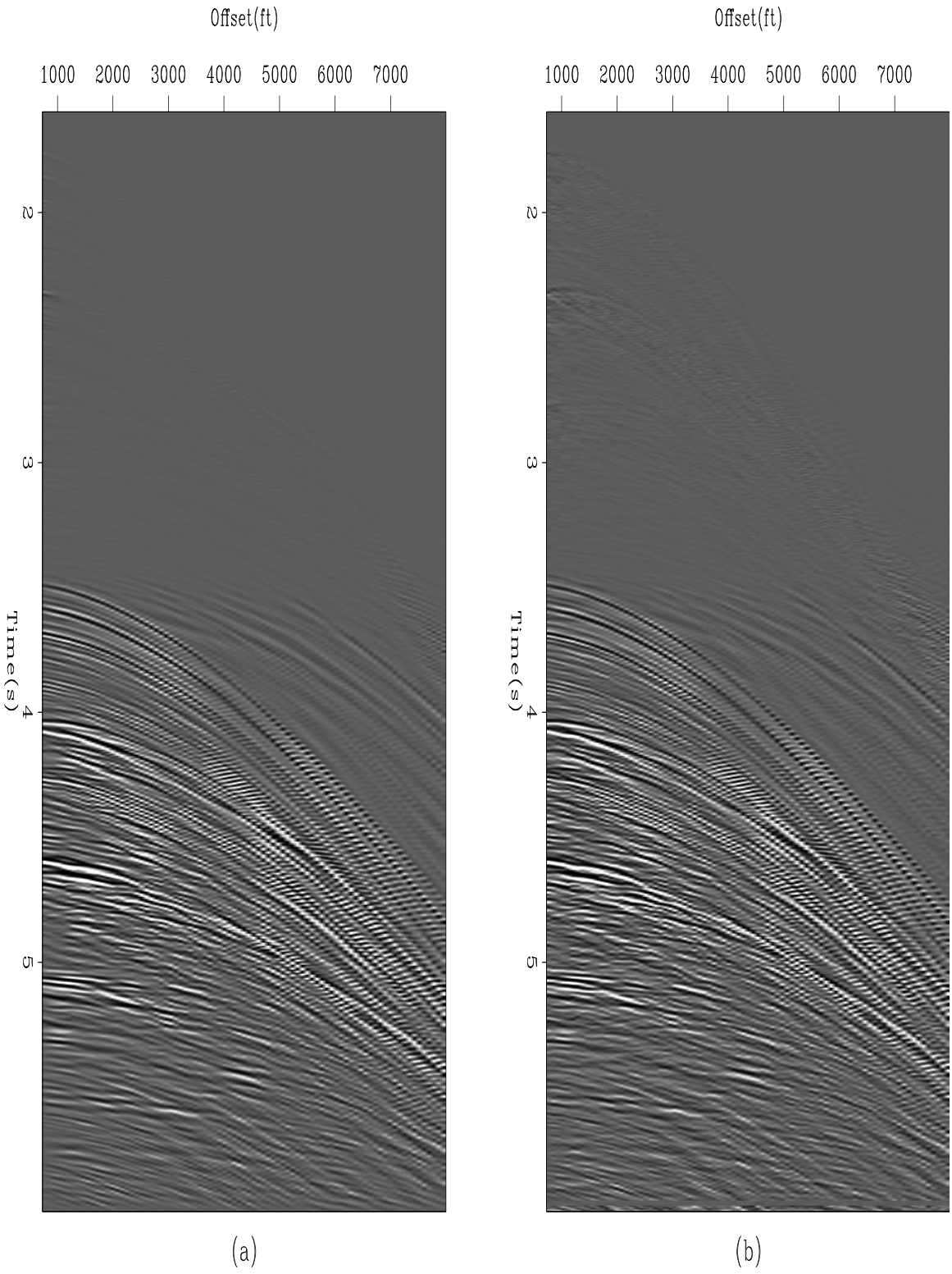

Figure 11: (a) The extracted multiples using the subtraction method. (b) The extracted multiples using the Wiener-like method. antoine2-noiz-400 [CR]

(2) that this new formulation leads to a proper subtraction of the noise components, and (3) that so far, this method is comparable in efficiency to the Wiener-like method. The first results are encouraging. Yet, we have not explored the possibilities offered by the regularization to improve the signal-noise separation.

ACKNOWLEDGMENTS

We thank WesternGeco and Saudi Aramco for providing the data.

REFERENCES

Abma, R., 1995, Least-squares separation of signal and noise with multidimensional filters: Ph.D. thesis, Stanford University.

Brown, M., and Clapp, R., 2000, (t,x) domain, pattern-based ground roll removal: 70th Annual International Meeting, Society Of Exploration Geophysicists, Annual Meeting Abstracts, 2115–2118.

Brown, M., Clapp, R. G., and Marfurt, K., 1999, Predictive signal/noise separation of groundroll-contaminated data: SEP–**102**, 111–128.

Castleman, K. R., 1996, Digital image processing: Prentice-Hall.

Claerbout, J., 1998, Multidimensional recursive filters via a helix: Geophysics, **63**, no. 05, 1532–1541.

Clapp, R. G., and Brown, M., 2000, $(t-x)$ domain, pattern-based multiple separation: SEP–**103**, 201–210.

Clapp, R. G., Fomel, S., Crawley, S., and Claerbout, J. F., 1999, Directional smoothing of non-stationary filters: SEP–**100**, 197–209.

Dragoset, W. H., and Jericevic, Z., 1998, Some remarks on surface multiple attenuation: Geophysics, **63**, no. 02, 772–789.

Fomel, S., 1997, On model-space and data-space regularization: A tutorial: SEP–**94**, 141–164.

Fomel, S., 2000, Applications of plane-wave destructor filters: SEP–**105**, 1–26.

Guitton, A., 1999, Multiple elimination using a pattern-recognition technique: The Leading Edge, **18**, no. 1, 92,94–98.

Guitton, A., 2001, Coherent noise attenuation: A synthetic and field example: SEP–**108**, 225–248.

Menke, W., 1989, Geophysical Data Analysis: Discrete Inverse Theory: Academic Press.

Nemeth, T., 1996, Imaging and filtering by least-squares migration: Ph.D. thesis, University of Utah.

Rickett, J., and Guitton, A., 2000, Multi-dimensional Fourier transforms in the helical coordinate system: SEP–**105**, 167–176.

Spitz, S., 1999, Pattern recognition, spatial predictability, and subtraction of multiple events: The Leading Edge, **18**, no. 1, 55–58.

Spitz, S., 2000, Model-based subtraction of multiple events in the frequency-space domain: 70th Annual International Meeting, Society Of Exploration Geophysicists, Annual Meeting Abstracts, 1969–1972.

Tarantola, A., 1987, Inverse Problem Theory: Elsevier Science Publisher.

Verschuur, D. J., Berkhout, A. J., and Wapenaar, C. P. A., 1992, Adaptive surface-related multiple elimination: Geophysics, **57**, no. 09, 1166–1177.

APPENDIX A

SURFACE-RELATED MULTIPLE PREDICTION THEORY

This section details how multiples are generated by convolution of shot gathers. For a 1-D earth, the convolution can be done directly in the $f-k$ domain. For a 2-D earth, the convolution becomes nonstationary. In addition, one convolution of the shot gathers tends to overpredict high-order multiples. If $p(g|s)$ represents a single frequency component of the primary reflected wavefield recorded at g after an impulsive shot at s, then the *first-order* surface-related multiple, $m(g|s)$, can be computed with a Kirchhoff-style integral over the reflection surface:

$$m(g|s) = \int p(g|g')\; p(g'|s)\; dg'. \tag{10}$$

Equation (10) is expensive to evaluate, especially for large 3-D data sets, but nevertheless widely-used for multiples modeling.

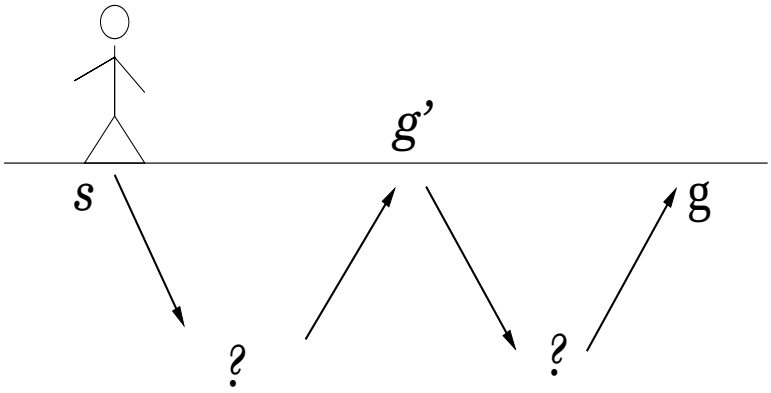

Figure 12: The wavefield is emitted at s and recorded at g. The multiple bounces somewhere at g'. antoine2-hombre [NR]

One-dimensional earth and impulsive source

Let's define u_0 as the primary wavefield and u_1 the surface-related, first-order multiple wavefield recorded at the surface. If the earth varies only as a function of depth, then u will not depend on both s and g, but only on the offset, $h = g - s$. In this one-dimensional case, equation (10) becomes

$$u_1(g-s) = \int u_0(g-g')\, u_0(g'-s)\, dg' \tag{11}$$

$$u_1(h) = \int u_0(h-h')\, u_0(h')\, dh', \tag{12}$$

where $h' = g' - s$. Equation (12) clearly represents a convolution, so can be computed by multiplication in the Fourier domain such that

$$U_1(k_h) = U_0(k_h)^2, \tag{13}$$

where $U_i(k_h)$ is the Fourier transform of $u_i(h)$ defined by

$$U_i(k_h) = \int u_i(h)\, e^{-2\pi i k_h h} dh. \tag{14}$$

Equation (13) can be extended to deal with a smoothly varying earth by considering common shot-gathers (or common midpoint gathers) independently, and assuming the earth is locally one-dimensional in the vicinity of the shot e.g., Rickett and Guitton (2000):

$$U_1(k_h, s) = U_0(k_h, s)^2. \tag{15}$$

Two-dimensional earth

In the general case, modeling multiples becomes more expensive. Equation (12) is not valid anymore (except for smoothly varying media), and the convolution becomes nonstationary (shot gathers are different from one location to another). Hence, the wavefield is not only a function of offset, h, but also depends on another spatial coordinate such as shot location s. Under this parameterization, equation (10) can be written as

$$u_1(h,s) = \int u_0(h-h', s+h')\, u_0(h', s)\, dh'. \tag{16}$$

Now, following Dragoset and Jericevic (1998), we introduce some amplitude corrections in the previous equation:

$$\begin{aligned} u_0(h-h', s+h') &= F_{t\to\omega}[\sqrt{t} u_0(h-h', s+h', t)], \\ u_0(h', s) &= (1-i)\sqrt{\frac{\omega}{4\pi}} F_{t\to\omega}[\sqrt{t} u_{0g}(h', s, t)]. \end{aligned} \tag{17}$$

Limitations of the multiple prediction using real data

In the real life, the source is not impulsive. In addition, multiples are computed directly from the data and not from the primary wavefield. Hence, the relative amplitude of first order multiples with respect to higher order multiples is not preserved. To illustrate this last point, consider the surface-related multiple modeling equation (Verschuur et al., 1992)

$$u_r = u_0 - W^{-1} u_m, \tag{18}$$

where u_r is the recorded wavefield at the surface, W the source wavelet, and u_m the multiple wavefield given by

$$\begin{aligned} u_m &= u_0 \otimes u_0 - W^{-1} u_0 \otimes u_0 \otimes u_0 \\ &\quad + W^{-2} u_0 \otimes u_0 \otimes u_0 \otimes u_0 \ldots \end{aligned} \tag{19}$$

$$u_m = u_1 + u_2 + u_3 + \ldots \tag{20}$$

where $\otimes$ represents the nonstationary convolution and u_i the i-th order multiples. If we use equation (16), replacing u_0 by u_r, we obtain for the approximated multiple field $\tilde{u}_m$

$$\tilde{u}_m = u_1 + 2u_2 + 3u_3 + \dots \tag{21}$$

Comparing equation (33) and equation (34), we notice that higher order multiples in equation (34) are multiplied by a coefficient that is difficult to correct for. Therefore higher order multiples have the correct kinematics, but the wrong amplitudes. Hence, our modeling scheme explicitely overpredict high-order multiples (amplitude wise) but models them with the correct pattern.

APPENDIX B

GEOMETRIC INTERPRETATION OF THE NOISE AND SIGNAL FILTERS

In this section, we give a geometric interpretation of the noise and data filters which appear in equation (5). The properties of the resolution operators are well known (Tarantola, 1987). Our goal is to extend these properties to the particular case of the subtraction scheme proposed in equation (5). But first, it is useful to give some definitions.

Definitions

We give a set of definitions that will help us to better understand the properties of the noise and signal filters in equation (5).

Definition 1: an operator **P** is a projector if

$$\mathbf{PP} = \mathbf{P}. \tag{22}$$

Definition 2: two operators **P** and **Q** are complementary operators if

$$\mathbf{P} + \mathbf{Q} = \mathbf{I}. \tag{23}$$

Definition 3: two operators **P** and **Q** are mutually orthogonal if

$$\mathbf{PQ} = \mathbf{QP} = \mathbf{0}. \tag{24}$$

Definition 4: the ℓ^2 norm of a vector **v** is

$$\|\mathbf{v}\|^2 = \sum_i v_i^2 \tag{25}$$

or

$$\|\mathbf{v}\|^2 = \mathbf{v}'\mathbf{v}, \tag{26}$$

where (') is the adjoint.
Definition 5: two vectors **u** and **v** are orthogonal if

$$\mathbf{u}'\mathbf{v} = \mathbf{v}'\mathbf{u} = 0. \tag{27}$$

General properties of the noise and signal filters

Following the preceding definitions, we can define the noise and signal filters more precisely. But first, remind that

$$\begin{pmatrix} \hat{\mathbf{m}}_\mathbf{n} \\ \hat{\mathbf{m}}_\mathbf{s} \end{pmatrix} = \begin{pmatrix} (\mathbf{L}_\mathbf{n}'\overline{\mathbf{R}_\mathbf{s}}\mathbf{L}_\mathbf{n})^{-1}\mathbf{L}_\mathbf{n}'\overline{\mathbf{R}_\mathbf{s}} \\ (\mathbf{L}_\mathbf{s}'\overline{\mathbf{R}_\mathbf{n}}\mathbf{L}_\mathbf{s})^{-1}\mathbf{L}_\mathbf{s}'\overline{\mathbf{R}_\mathbf{n}} \end{pmatrix} \mathbf{d},$$

with

$$\begin{aligned} \overline{\mathbf{R_s}} &= \mathbf{I} - \mathbf{L_s}(\mathbf{L_s'L_s})^{-1}\mathbf{L_s'}, \\ \overline{\mathbf{R_n}} &= \mathbf{I} - \mathbf{L_n}(\mathbf{L_n'L_n})^{-1}\mathbf{L_n'}. \end{aligned} \tag{28}$$

$\overline{\mathbf{R_s}}$ and $\overline{\mathbf{R_n}}$ are signal and noise filtering operators respectively. If we denote

$$\begin{aligned} \overline{\mathbf{R_s}} &= \mathbf{I} - \mathbf{R_s}, \\ \overline{\mathbf{R_n}} &= \mathbf{I} - \mathbf{R_n}. \end{aligned} \tag{29}$$

with $\mathbf{R_s} = \mathbf{L_s}(\mathbf{L_s'L_s})^{-1}\mathbf{L_s'}$ and $\mathbf{R_n} = \mathbf{L_n}(\mathbf{L_n'L_n})^{-1}\mathbf{L_n'}$ the signal and noise resolution operators, we deduce that $\mathbf{R_s}$ and $\overline{\mathbf{R_s}}$, $\mathbf{R_s}$ and $\overline{\mathbf{R_s}}$ are complementary operators (definition 2).

It can be shown that $\overline{\mathbf{R_s}}$, $\overline{\mathbf{R_n}}$, $\mathbf{R_s}$ and $\mathbf{R_n}$ are projectors. For $\mathbf{R_s}$ and $\overline{\mathbf{R_s}}$, we have

$$\begin{aligned} \mathbf{R_sR_s} &= \mathbf{L_s}(\mathbf{L_s'L_s})^{-1}\mathbf{L_s'L_s}(\mathbf{L_s'L_s})^{-1}\mathbf{L_s'}, \\ &= \mathbf{L_s}(\mathbf{L_s'L_s})^{-1}\mathbf{L_s'}, \\ \mathbf{R_sR_s} &= \mathbf{R_s}, \end{aligned} \tag{30}$$

and

$$\begin{aligned} \overline{\mathbf{R_s}}\,\overline{\mathbf{R_s}} &= (\mathbf{I} - \mathbf{R_s})(\mathbf{I} - \mathbf{R_s}), \\ &= \mathbf{I} - 2\mathbf{R_s} + \mathbf{R_s}, \\ \overline{\mathbf{R_s}}\,\overline{\mathbf{R_s}} &= \overline{\mathbf{R_s}}. \end{aligned} \tag{31}$$

Thus, $\mathbf{R_s}$ and $\overline{\mathbf{R_s}}$ are projectors as defined in definition 1. The same proofs work for $\mathbf{R_n}$ and $\overline{\mathbf{R_n}}$.

We can prove that $\overline{\mathbf{R_s}}$ and $\mathbf{R_s}$, $\overline{\mathbf{R_n}}$ and $\mathbf{R_n}$ are mutually orthogonal. For $\mathbf{R_s}$ and $\overline{\mathbf{R_s}}$, we have

$$\begin{aligned} \overline{\mathbf{R_s}}\mathbf{R_s} &= (\mathbf{I} - \mathbf{R_s})\mathbf{R_s}, \\ &= (\mathbf{R_s} - \mathbf{R_s}), \\ \overline{\mathbf{R_s}}\mathbf{R_s} &= \mathbf{0}. \end{aligned} \tag{32}$$

Hence, $\overline{\mathbf{R_s}}$ and $\mathbf{R_s}$, $\overline{\mathbf{R_n}}$ and $\mathbf{R_n}$ are complementary, mutually orthogonal projectors.

Geometric interpretation

The operators $\mathbf{R_n}$ and $\mathbf{R_s}$ are the noise and signal resolution operators. They describe how well the predictions match the noise and signal (Menke, 1989). In the following equations, we consider that

$$\mathbf{R_n n} = \mathbf{n} \tag{33}$$

and

$$\mathbf{R_s s} = \mathbf{s}, \tag{34}$$

meaning that each component of the data has been predicted. These equalities will help us to build a comprehensive geometric interpretation for the different operators. Based on equations (33) and (34), we have for the data vector $\mathbf{d}$ the following equalities:

$$\begin{aligned} \mathbf{R_s d} &= \mathbf{R_s n} + \mathbf{s} \\ \mathbf{R_n d} &= \mathbf{R_n s} + \mathbf{n}, \end{aligned} \tag{35}$$

and

$$\begin{aligned} \overline{\mathbf{R_s}}\mathbf{d} &= \overline{\mathbf{R_s}}\mathbf{n} \\ \overline{\mathbf{R_n}}\mathbf{d} &= \overline{\mathbf{R_n}}\mathbf{s}. \end{aligned} \tag{36}$$

In the following equations, we prove that $\|\overline{\mathbf{R_n}}\mathbf{s}\|^2 + \|\mathbf{R_n s} + \mathbf{n}\|^2 = \|\mathbf{d}\|^2$:

$$\begin{aligned} \|\overline{\mathbf{R_n}}\mathbf{s}\|^2 + \|\mathbf{R_n s} + \mathbf{n}\|^2 &= \mathbf{s}'\overline{\mathbf{R_n}}'\overline{\mathbf{R_n}}\mathbf{s} + \mathbf{s}'\mathbf{R_n}'\mathbf{R_n}\mathbf{s} + \mathbf{s}'\mathbf{R_n}'\mathbf{n} + \mathbf{n}'\mathbf{R_n}\mathbf{s} + \\ &\quad \mathbf{n}'\mathbf{n} \\ &= \mathbf{d}'\overline{\mathbf{R_n}}\mathbf{d} + \mathbf{s}'\mathbf{R_n}\mathbf{s} + \mathbf{n}'\mathbf{R_n}\mathbf{s} + \mathbf{s}'\mathbf{R_n}\mathbf{n} + \\ &\quad \mathbf{n}'\mathbf{R_n}\mathbf{n} \\ &= \mathbf{d}'\overline{\mathbf{R_n}}\mathbf{d} + \mathbf{d}'\mathbf{R_n}\mathbf{d} \\ &= \mathbf{d}'\mathbf{d} \\ \|\overline{\mathbf{R_n}}\mathbf{s}\|^2 + \|\mathbf{R_n s} + \mathbf{n}\|^2 &= \|\mathbf{d}\|^2. \end{aligned} \tag{37}$$

Similarly, we have $\|\overline{\mathbf{R_s}}\mathbf{n}\|^2 + \|\mathbf{R_s n} + \mathbf{s}\|^2 = \|\mathbf{d}\|^2$. If we use equations (35) and (36), the last two equalities can be written as follows:

$$\begin{aligned} \|\overline{\mathbf{R_n}}\mathbf{d}\|^2 + \|\mathbf{R_n d}\|^2 &= \|\mathbf{d}\|^2, \\ \|\overline{\mathbf{R_s}}\mathbf{d}\|^2 + \|\mathbf{R_s d}\|^2 &= \|\mathbf{d}\|^2. \end{aligned} \tag{38}$$

Hence, $\overline{\mathbf{R_n}}\mathbf{d}$, $\mathbf{R_n d}$ and $\mathbf{d}$ form a right triangle with hypotenuse $\mathbf{d}$ and legs $\overline{\mathbf{R_n}}\mathbf{d}$ and $\mathbf{R_n d}$, as depicted in Figure 13; similarly, $\overline{\mathbf{R_s}}\mathbf{d}$, $\mathbf{R_s d}$ and $\mathbf{d}$ form a right triangle with hypotenuse $\mathbf{d}$ and legs $\overline{\mathbf{R_s}}\mathbf{d}$ and $\mathbf{R_s d}$. If $\mathbf{n}$ and $\mathbf{s}$ are orthogonal, $\mathbf{s}$ is in the null space of $\mathbf{R_n}$ and $\overline{\mathbf{R_n}}\mathbf{d} = \overline{\mathbf{R_n}}\mathbf{s} = \mathbf{s}$ (Figure 14). Similarly, $\mathbf{n}$ is in the null space of $\mathbf{R_s}$ and $\overline{\mathbf{R_s}}\mathbf{d} = \overline{\mathbf{R_s}}\mathbf{n} = \mathbf{n}$.

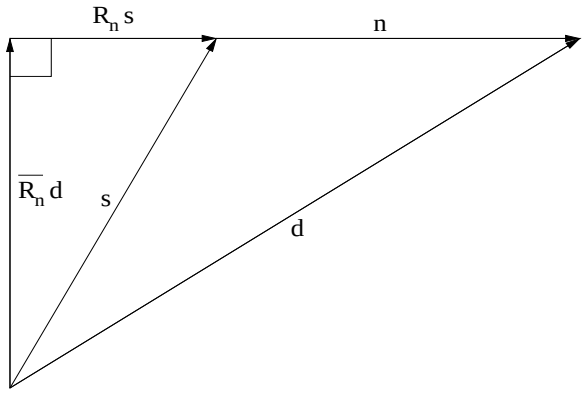

Figure 13: A geometric interpretation of the noise filter when $\mathbf{n}$ and $\mathbf{s}$ are not orthogonal. antoine2-geom11 [NR]

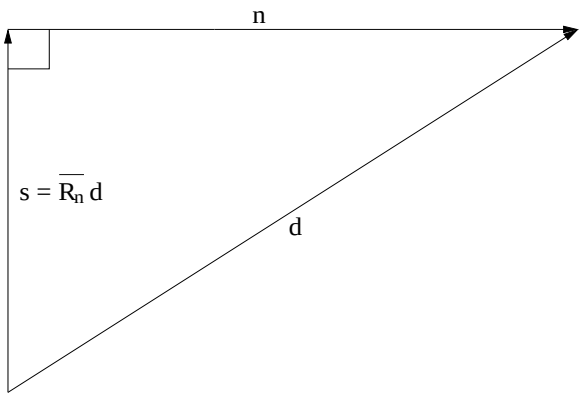

Figure 14: A geometric interpretation of the noise filter when **n** and **s** are orthogonal. antoine2-geom21 [NR]